

Application of Ba_{0.5}Sr_{0.5}TiO₃ (Bst) Film Doped with 0%, 2%, 4% and 6% Concentrations of RuO₂ as an Arduino Nano-Based Bad Breath Sensor

by Mochamad Zakki Fahmi

Submission date: 01-Sep-2021 08:47PM (UTC+0800)

Submission ID: 1639428963

File name: A31-Application_of_Ba_{0.5}Sr_{0.5}TiO₃_Bst_Film_Doped_with.pdf (3.32M)

Word count: 5946

Character count: 42108

Article

Application of Ba_{0.5}Sr_{0.5}TiO₃ (Bst) Film Doped with 0%, 2%, 4% and 6% Concentrations of RuO₂ as an Arduino Nano-Based Bad Breath Sensor

Irzaman ^{1,*}, Ridwan Siskandar ², Brian Yulianto ³ , Mochammad Zakki Fahmi ⁴ and Ferdiansjah ⁵¹ Physics Department, IPB University, Bogor, West Java 16680, Indonesia² Computer Engineering Study Program, College of Vocational Studies, IPB University, Bogor, West Java 16151, Indonesia; ridwansiskandar@gmail.com or ridwansiskandar@apps.ipb.ac.id³ Engineering Physics Department, Bandung Institute of Technology, Bandung, West Java 40132, Indonesia; brian@tf.itb.ac.id⁴ Chemistry Department, Airlangga University, Surabaya, East Java 60115, Indonesia; m.zakki.fahmi@fst.unair.ac.id⁵ Nuclear and Technical Physics Department, Gadjah Mada University, Yogyakarta 55281, Indonesia; ferdiansjah@ugm.ac.id

* Correspondence: irzaman@apps.ipb.ac.id

Received: 16 October 2019; Accepted: 13 December 2019; Published: 25 December 2019



Abstract: Ba_{0.5}Sr_{0.5}TiO₃ (BST) film doped with variations in RuO₂ concentration (0%, 2%, 4%, and 6%) has been successfully grown on a type-p silicon substrate (100) using the chemical solution deposition (CSD) method and spin-coating at a speed of 3000 rpm for 30 s. The film on the substrate was then heated at 850 °C for 15 h. The sensitivity of BST film + RuO₂ variations as a gas sensor were characterized. The sensitivity characterization was assisted by various electronic circuitry with the purpose of producing a sensor that is very sensitive to gas. The responses from the BST film + RuO₂ variation were varied, depending on the concentration of the RuO₂ dope. BST film doped with 6% RuO₂ had a very good response to halitosis gases; therefore, this film was applied as the Arduino-Nano-based bad-breath detecting sensor. Before it was integrated with the microcontroller, the voltage output of the BST film was amplified using an op-amp circuit to make the voltage output from the BST film readable to the microcontroller. The changes in the voltage response were then shown on the prototype display. If the voltage output was ≤12.9 mV, the display would read “bad breath”. If the voltage output >42.1 mV, the display would read “fragrant”. If 12.9 mV < voltage output ≤ 42.1 mV, the display would read “normal”.

Keywords: Ba_{0.55}Sr_{0.45}TiO₃ (BST) film; RuO₂; bad breath gas sensor; op-amp; Arduino Nano

1. Introduction

Halitosis is a general term to describe the presence of an unpleasant odor when exhaling [1]. Halitosis is caused by food debris left in the mouth, which is processed by the normal flora in the oral cavity, such as protein hydrolysis by Gram-negative bacteria [2,3]. Oral conditions such as the decreased flow of saliva, the blocked flow of saliva, the increase in the number of anaerobic Gram-negative bacteria, the increase in food proteins, a more-alkaline oral cavity pH, and an increased number of dead and necrotic cells in the mouth could also trigger bad breath [4].

The discovery of volatile sulfur compounds (VSCs) which are believed to be the main cause of halitosis has piqued the interest of many researchers in conducting studies related to them. VSCs are a product of anaerobic bacterial activities and react with protein in the mouth from food debris that contains protein, dead blood cells, dead bacteria, or epithelial cells which have sloughed off

the oral mucosa [1]. VSCs are volatile sulfuric compounds which are formed through bacterial reactions (especially anaerobic bacteria) with proteins, which are broken down into amino acids. There are three amino acids that produce VSCs, cysteine, which produces hydrogen sulfide (H_2S), methionine, which produces methyl mercaptan (CH_3SH), and cystine, which produces dimethyl Sulfide (CH_3SCH_3) [5].

Ferroelectric materials have the ability to change the direction of their internal electric currents, can be spontaneously polarized, and demonstrate a hysteresis effect which is related to dielectric shifts in responding to the internal electricity field [1–3]. The hysteresis properties and high dielectric constant can be applied to the dynamic random access memory (DRAM) cell with a storage capacity of over 1 Gbit; the piezoelectric properties can be utilized as a microactuator and sensor; the pyroelectric properties can be applied in the infrared sensor; the electro-optic properties can be applied in the infrared thermal switch; and the polarizability can be applied as a non-volatile ferroelectric random access memory (NVRAM) [6–8].

BST film can be produced using fairly simple equipment on a tight budget and in relatively short time [9–11]. In the film-producing process, there are a number of methods that could be used such as the metalorganic chemical vapor deposition (MOCVD) method [12–14], the chemical vapor deposition method [15], the sol-gel method [16–19], the atomic layer deposition (ALD) method [20], the pulsed laser ablation deposition (PLAD) method [21,22], rf sputtering [17,23,24], and chemical solution deposition (CSD) method [24–31]. The CSD method is superior as it can control the film stoichiometry with good quality, an easy procedure, and has a fairly affordable cost [32–34]. The CSD method is a method of making thin films by deposition of a chemical solution onto a substrate then preparation through spin-coating at a certain rotational speed [35]. The CSD method has long been developed for growing thin film perovskite, since the 1980s [36].

2. Research Method

2.1. Preparation of the Type-p Silicon (100) Substrate

The substrate used was type-p silicon (100). The substrate was cut into 4 squares sized 1×1 cm as seen in Figure 1. After cutting, the substrate was washed with 5% hydrofluoric acid (HF) mixed with 2% aquadest [37].

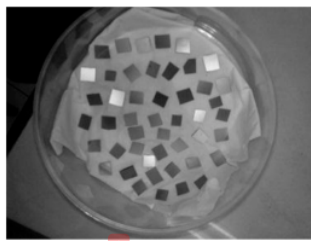


Figure 1. The type-p silicon (100) substrate cut into 1×1 cm² squares.

2.2. Preparation of the $Ba_{0.5}Sr_{0.5}TiO_3$ Film Doped with RuO_2 Solution

The $Ba_{0.5}Sr_{0.5}TiO_3$ solution doped with RuO_2 0%, 2%, 4% and 6% grown on the substrate using the CSD method was made from 0.3512 g of barium acetate [$Ba(CH_3COOH)_2$, 99%], 0.2314 g of strontium acetate [$Sr(CH_3COOH)_2$, 99%], 0.7105 g of titanium isopropoxide [$Ti(C_12O_4H_{28})$, 99%], and 2.5 mL of 2-methoxyethanol [$H_3COOCH_2CH_2OH$, 99%] as the solvent, and all the ingredients were then sonicated in a Branson model 2210 sonicator for 1 h (the resulting mixture is called the precursor) [38].

2.3. Growing the $Ba_{0.5}Sr_{0.5}TiO_3$ Film Doped with RuO_2

The film-growing process was conducted using a spin-coating reactor, where the type-p silicon substrate that had been washed was placed on the spin coating reactor plate which had had a piece of double-sided tape affixed to the center. Next, 1/3 of the surface of the type-p silicon substrate that had been affixed to the spin coating reactor plate surface was covered with seal tape. The seal tape was used to prevent the type-p silicon substrate surface from being entirely covered by the BST solution, and the double-sided tape was used to make sure the substrate did not slip off the plate when the spin-coating reactor was operated.

The substrate that had been placed on the spin-coating reactor plate was dripped upon with 3 drops of BST solution, then the spin-coating reactor was spun at 3000 rpm for 30 s. The dripping process was repeated 3 times with a 60-second gap between each repeat. After dripping, the substrate was collected using tweezers [37]. Process Growing the $Ba_{0.5}Sr_{0.5}TiO_3$ Film Doped with RuO_2 shown in Figure 2.



Figure 2. Process Growing the $Ba_{0.5}Sr_{0.5}TiO_3$ Film Doped with RuO_2 .

2.4. The Annealing Process

The purpose of the annealing process was to diffuse the BST solution with the substrate. The annealing process was conducted gradually using a VulcanTM-3-130 model furnace. The heating began at room temperature and was raised to the required annealing temperature, 850 °C, with an adjusted temperature rise (1.7 °C/min), and then the annealing temperature was maintained for 15 h. Next, furnace cooling was conducted until room temperature was reached again [37]. The annealing process can be seen in Figure 3.

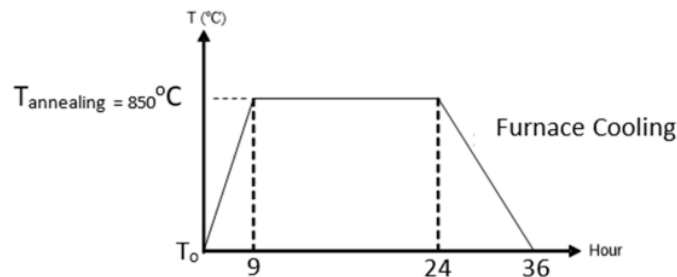


Figure 3. The annealing process.

2.5. Contact Installation in the $Ba_{0.5}Sr_{0.5}TiO_3$ Film Doped with RuO_2

The contact holes in the film were made as 2×2 mm squares on the BST layer and the remaining part of the BST film was covered using aluminum foil. The next process was aluminum (Al) metallization as the contact medium for the film which was done by evaporation in a vacuum container. And then the holder and thin copper wire were affixed using silver paste [37]. The process of aluminum metallization as the film's contact medium can be seen in Figure 4. The $Ba_{0.5}Sr_{0.5}TiO_3$ film doped with RuO_2 model,

the result of the copper wire installation, and the physical appearance of the $Ba_{0.5}Sr_{0.5}TiO_3$ film doped with RuO_2 and the physical appearance of the $Ba_{0.5}Sr_{0.5}TiO_3$ film doped with RuO_2 can be seen in Figure 5.

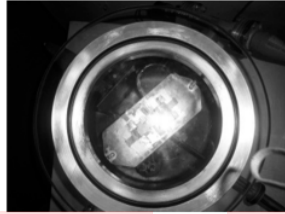
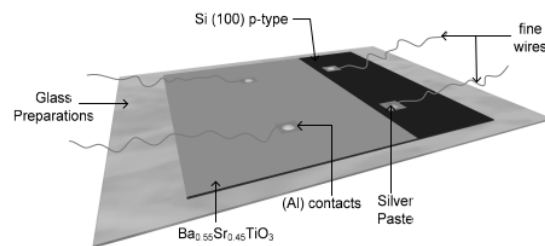


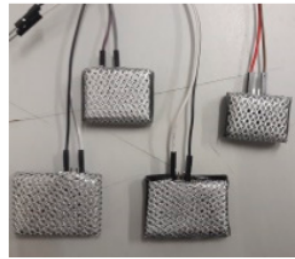
Figure 4. The aluminum metallization process as the film's contact medium.



(a)



(b)



(c)

Figure 5. (a) The $Ba_{0.5}Sr_{0.5}TiO_3$ film doped with RuO_2 model; (b) The result of the copper wire installation; (c) The physical appearance of the $Ba_{0.5}Sr_{0.5}TiO_3$ film doped with RuO_2 .

2.6. Characterization of the $Ba_{0.5}Sr_{0.5}TiO_3$ Film Doped with RuO_2 as a Bad Breath-Gas Sensor

Characterization of the $Ba_{0.5}Sr_{0.5}TiO_3$ film doped with RuO_2 included characterization of its sensitivity as a bad breath-gas sensor. The sensitivity of $Ba_{0.5}Sr_{0.5}TiO_3$ film doped with RuO_2 as a bad breath-gas sensor was demonstrated by the difference in output voltage and the input voltage (exposure to halitosis gases), $(\Delta V/\Delta G)$, with V as the output voltage and G the input voltage with exposure to halitosis gases. The greater the voltage difference, the more sensitive the film is considered to be.

2.7. Equipment Design

The prototype was designed to be portable. The prototype design was 7 cm in length, with a 6-cm-diameter handle, 3-cm-diameter lid, and 1-cm height, and the $Ba_{0.5}Sr_{0.5}TiO_3$ film doped with RuO_2 itself was $2 \times 3 \text{ cm}^2$. These measurements were made according to the requirements of the

electronic components contained by the prototype design. The prototype design sketch can be seen in Figure 6.

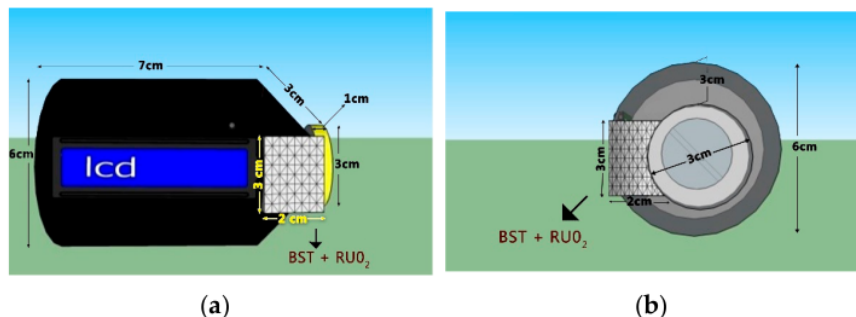


Figure 6. The prototype design: (a) front view; (b) Side view.

The components used in the bad-breath detector prototype consisted of the input component, the processing component, and output component. The input component is shown in Figure 7, label 'a', the $Ba_{0.5}Sr_{0.5}TiO_3$ film doped with RuO_2 6%. The processing component used a 10-bit microcontroller (Figure 7, labeled 'b'), the ATmega138/Arduino Nano which is $3 \times 1 \text{ cm}^2$ in size. The output component (Figure 7, labeled 'c' and 'd'), the LED as the indicator and an LCD as the voltage value and breath odor condition display.

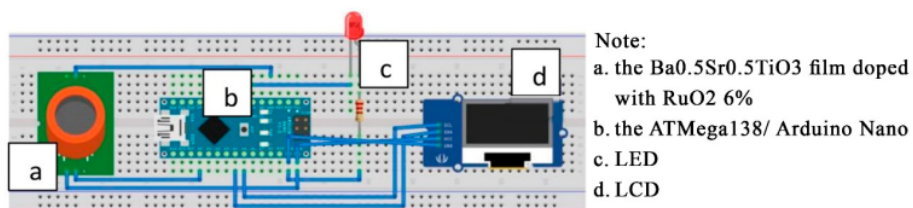


Figure 7. Sketch of the prototype's electronic circuitry.

3. Results and Discussion

3.1. Characterization of the $Ba_{0.5}Sr_{0.5}TiO_3$ Film Doped with RuO_2 as a Bad Breath-Gas Sensor

The measurements were taken by two methods: variation in the distance of odor exposure to the film position and variations in oral hygiene conditions. Variations in the distance between odor exposure to the film position were conducted at distances of 2 cm, 4 cm, 6 cm and 8 cm with bad breath exposure which was considered stable (exhalations from the mouth). Variations in oral hygiene were conducted before the oral cavity was cleaned (straight out of bed) and after it was cleaned (after brushing teeth).

Tables 1 and 2 present the voltage output measurement data of $Ba_{0.5}Sr_{0.5}TiO_3$ film doped with RuO_2 (after being stabilized with a Wheatstone circuit and amplified with an op-amp). The Wheatstone circuit and op-amp for the $Ba_{0.5}Sr_{0.5}TiO_3$ film doped with RuO_2 are shown in Figure 8.

Table 1. The voltage output measurement data of $Ba_{0.5}Sr_{0.5}TiO_3$ film doped with RuO_2 as a bad breath gas sensor with variations in the gas exposure distance: 2 cm, 4 cm, 6 cm and 8 cm.

$Ba_{0.5}Sr_{0.5}TiO_3$ Film with Variations in RuO_2 Dope (%)	Output Voltage at 2 cm Exposure (mV)	Output Voltage at 4 cm Exposure (mV)	Output Voltage at 6 cm Exposure (mV)	Output Voltage at 8 cm Exposure (mV)
0	12.5	12.4	12.4	12.4
2	12.5	12.5	12.1	-
4	16.9	14.4	-	-
6	29.0	27.7	26.4	20.3

Table 2. Voltage difference measurement data of $Ba_{0.5}Sr_{0.5}TiO_3$ film doped with RuO_2 in various oral conditions.

$Ba_{0.5}Sr_{0.5}TiO_3$ Film with Variations in RuO_2 Dope (%)	Film Output Voltage			ΔV before and after Cleaning (mV)
	before Cleansing (Straight out of Bed) (mV)	after Cleansing (after Brushing Teeth) (mV)	after 15 min after (after Brushing Teeth+Eat) (mV)	
0	12.4	12.7	12.7	0.3
2	11.3	12.5	12.4	1.2
4	13.6	17.9	17.8	4.3
6	12.9	42.1	41.9	29.2

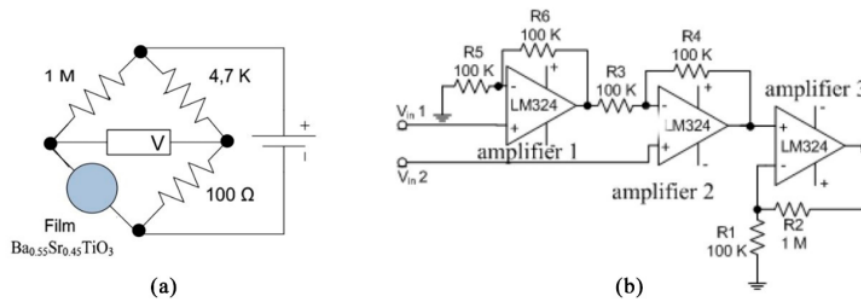


Figure 8. (a) The Wheatstone circuit; (b) The op-amp circuit.

Table 1 presents voltage output measurement data with variations in halitosis gas exposure distance of $Ba_{0.5}Sr_{0.5}TiO_3$ film with doped with varied RuO_2 concentrations. Table 2 presents the output voltage with a variety of oral conditions (halitosis-gas input) of the $Ba_{0.5}Sr_{0.5}TiO_3$ film doped with varied RuO_2 concentrations.

The measurements in Table 1 aimed to evaluate the film's output voltage at distances of 2 cm, 4 cm, 6 cm, and 8 cm. The response revealed whether or not the $Ba_{0.5}Sr_{0.5}TiO_3$ film doped with RuO_2 gave a good response. The measurements presented in Table 2 were made by comparing the film's output voltage based on the film's response to oral conditions. The difference between the oral condition output (ΔV) was then used as proof that the film has a good sensitivity to halitosis gas. The best sensitivity was demonstrated by $Ba_{0.5}Sr_{0.5}TiO_3$ film doped with 6% RuO_2 . This film was then applied as the Arduino Nano-based bad breath gas detecting sensor.

Table 2 indicates that bad breath after cleaning (after brushing your teeth) and odor after 15 min after brushing your teeth + eating produce output values that do not differ much. It suggests that the condition read by the $Ba_{0.5}Sr_{0.5}TiO_3$ film doped with RuO_2 6% is not the odor from the toothpaste, but the bad breath from the bad breath gas in the oral cavity.

$Ba_{0.5}Sr_{0.5}TiO_3$ film doped with RuO_2 had a resistance of approximately $10^6\ \Omega$. By determining the values of R_1 and R_3 , the value of R_2 could be obtained using the equation $R_1 \cdot R_3 = R_2 \cdot R_4$.

The steps to finding the value of R_2 were: First, the value of R_1 and R_3 were determined to be $1\text{ M}\Omega$ and $100\ \Omega$. Second, initially, R_2 in the Wheatstone bridge circuit used a $100\text{ K}\Omega$ potentiometer which was done in order to make the V in potentiometer 0 volts. Then the potentiometer was disconnected

and the resistance in the potentiometer was measured using a multimeter. The value displayed by the multimeter was the resistance value used as R_2 . The resistance displayed was 4.68 K; therefore, $R_2 = 4.7$ K. The measurements were taken at the first and third terminals of the potentiometer.

The voltage signal emitted by the Wheatstone bridge was amplified by the op-amp circuit. The microcontroller used was the ATmega168 (which is also known as the Arduino Nano) which had a 10-bit resolution and a reference voltage of 4.8 volts; therefore, the microcontroller could differentiate between incoming voltages of 0.0046875 volts. To adjust the resolution of the $Ba_{0.5}Sr_{0.5}TiO_3$ film doped with RuO_2 to the ADC resolution, an amplifying circuit (op-amp) was employed. The amplifying circuit used in this study was a differential amplifying circuit and a non-inverting amplifying circuit, depicted in Figure 8b. A differential amplifying circuit is a circuit that compares two inputs. The differential amplifying circuit used was a combination between non-inverting and inverting circuits. The total circuit amplification for the BST film was 2 times amplification from the differential amplifying circuit and 11 times amplification from the non-inverting amplifying circuit, so the total amplification was 22 times. The mathematical calculations are represented by Equations (1) and (2).

Equation (1). The size of the amplification for the differential amplifying circuit was:

$$\frac{V_{out}}{V_{in}} = \left(1 + \frac{R_f}{R_{in}}\right) \left(\frac{R_f}{R_{in}}\right), \quad (1)$$

$$\frac{V_{out}}{V_{in}} = \left(1 + \frac{R_6}{R_5}\right) \left(\frac{R_4}{R_3}\right),$$

$$\frac{V_{out}}{V_{in}} = \left(1 + \frac{100K}{100K}\right) \left(\frac{100K}{100K}\right),$$

$$\frac{V_{out}}{V_{in}} = 2 \text{ times.}$$

Equation (2). The size of the amplification for the non-inverting amplifying circuit (amplifier 3) was:

$$\frac{V_{out}}{V_{in}} = \left(1 + \frac{R_f}{R_{in}}\right), \quad (2)$$

$$\frac{V_{out}}{V_{in}} = \left(1 + \frac{R_2}{R_1}\right),$$

$$\frac{V_{out}}{V_{in}} = \left(1 + \frac{1M}{100K}\right),$$

$$\frac{V_{out}}{V_{in}} = 11 \text{ times.}$$

The total amplification of the sensor's circuit was 22 times.

3.2. The Atmega168/Arduino Nano Microcontroller Circuit

The controlling circuit in the bad breath detector prototype was a 10-bit ATMEGA168 microcontroller. The output voltage from the best film circuit was the input signal for the microcontroller.

The input for the microcontroller from the best film was PORTA.0. LCD assisted by the IIC module; therefore, only two 2 PORTs: PORTA.4 for SDA and PORTA.5 for SCL. The digital PIN 3 was used for the LED indicator.

3.3. Testing the Entire System

Halitosis is generally caused by bacteria that develop naturally in the mouth. These bacteria produce sulfur-containing gases. As a result, during exhalation through the mouth, a pungent odor of sulfurous gases is emitted. These gases are the focus of the detection capabilities of this device.

The operating principle of the device is that when the power source (5 volts) is activated, the power source provides the input voltage needed by every circuit used. When the $\text{Ba}_{0.5}\text{Sr}_{0.5}\text{TiO}_3$ film doped with RuO_2 6% receives a stimulus in the form of bad breath, the ATmega168/Arduino Nano microcontroller gives a command to the LED and LCD.

If the $\text{Ba}_{0.5}\text{Sr}_{0.5}\text{TiO}_3$ film doped with RuO_2 6% receives a stimulus in the form of bad breath (voltage output ≤ 12.9 mV), the microcontroller will command the LED to turn on (as an indicator of bad breath) and the LCD will display the output values in the form of the voltage on the first line and the “bad breath” condition on the second line of the LCD. On the other hand, if the $\text{Ba}_{0.5}\text{Sr}_{0.5}\text{TiO}_3$ film doped with RuO_2 6% receives a stimulus in the form of “not bad breath” (voltage output > 42.1 mV), the microcontroller will give a command to the LED to remain turned off (as an indicator that the mouth is not malodorous) and the LCD will display an output in the form of the voltage on the first line of the LCD and the word “fragrant” on the second line.

If the $\text{Ba}_{0.5}\text{Sr}_{0.5}\text{TiO}_3$ film doped with RuO_2 6% receives a stimulus in the form of bad breath (12.9 mV $<$ voltage output ≤ 42.1 mV), the microcontroller will give a command to the LED to not turn on (as an indicator that the mouth is in a normal condition) and the LCD will display an output in the form of the voltage on the first line of the LCD and the word “normal” on the second line. The results of the bad breath, normal, and fragrant conditions are presented in Figure 9.

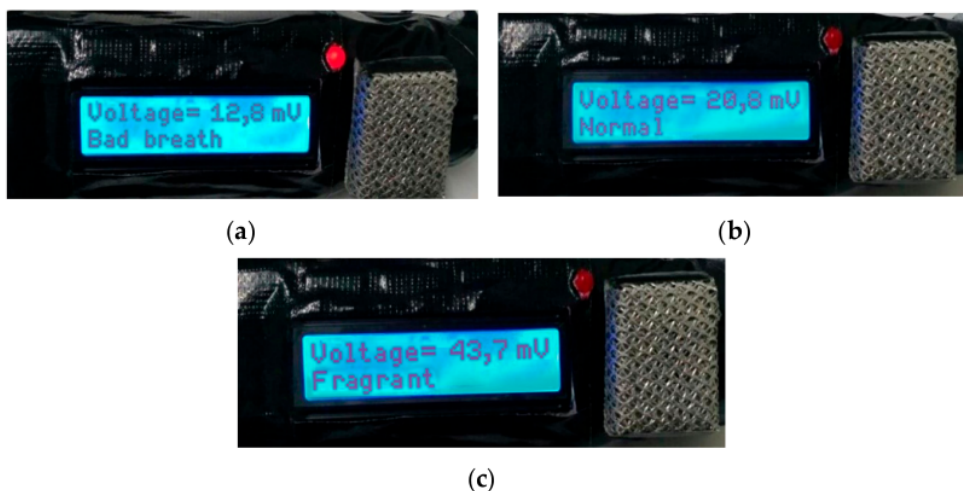


Figure 9. (a) The results of the testing at a “Bad breath” oral condition; (b) the results of the testing at a “Normal” oral condition; (c) The results of the testing at a “Fragrant” oral condition.

The MQ 136 sensor is a semiconductor component that functions as an odorant for tin oxide gas (SnO_2). The MQ 136 gas sensor has a high sensitivity to SO_2 . The MQ 136 can also be used to detect other vapors containing sulfur. Table 3 shows that the $\text{Ba}_{0.5}\text{Sr}_{0.5}\text{TiO}_3$ film with 6% RuO_2 doping variation shows the average accuracy of the tool is $\sim 99\%$ measured against the MQ 136 sensor. This proves that the $\text{Ba}_{0.5}\text{Sr}_{0.5}\text{TiO}_3$ film testing with the 6% RuO_2 doping variation shown in Figure 9 provides an objective result when reading bad breath.

Table 3. Measurement data of the accuracy of the voltage value between $\text{Ba}_{0.5}\text{Sr}_{0.5}\text{TiO}_3$ film RuO_2 6% doped relative to the commercially manufactured gas sensor (MQ 136) when detecting the odor conditions of the oral cavity.

	Output Voltage		
	before Cleansing (Straight out of Bed) (mV)	after Cleansing (after Brushing Teeth) (mV)	after 15 min after (after Brushing Teeth + Eat) (mV)
$\text{Ba}_{0.5}\text{Sr}_{0.5}\text{TiO}_3$ film with 6% doping variations	12.9	42.1	41.9
Gas sensor, manufacturer's product (MQ 136)	12.7	42.4	42.2
ΔV (mV)	0.2	0.3	0.3
Accuracy (%)	98.4	99.3	99.3

This tool is made to facilitate user detection of bad breath, so this portable unit can be carried everywhere by the user. The dimensions of the tool are shown in Figure 6. The position of the sensor is right inside the packaging container such as a microphone. Users can use the tool by: (1) activating the switch to the 'on' position; (2) the user blows the microphone in which there is a mouth odor sensor. Input in the form of bad breath will be read and processed by the microcontroller. The results of the microcontroller processing will be displayed on the 16×2 LCD as shown in Figure 9.

Figures 6a and 9 show that this device is built to provide user safety from electricity. Besides using only DC power supplies, the electronic components are housed inside a packaging container made of an insulating type material, ensuring user safety from electricity. The RuO_2 doped $\text{Ba}_{0.5}\text{Sr}_{0.5}\text{TiO}_3$ film cover container is also shock-resistant from saliva and toxins. If the mouth or saliva touches the RuO_2 doped $\text{Ba}_{0.5}\text{Sr}_{0.5}\text{TiO}_3$ film cover container it will not provide any electrical response because the container is coated with an insulating material, making it very safe.

Halitosis is a medical term for bad breath. Halitosis is a very common condition. According to the American Dental Association, at least 50 percent of adults around the world have bad breath. So generally, many do not realize that they have this condition.

One recent innovation for oral hygiene has been presented before. the innovation was called Breathometer Mint. The tool is used to monitor the user's mouth odor. With this tool, the user can find out whether the condition of the oral cavity is in good or bad condition. This device is integrated with applications on smartphones that will provide information about the user's oral cavity. Its use is quite practical, the tool is simply inserted into the mouth, then the user can exhale through his or her mouth. Then the Breathometer will detect the level of bacteria in the mouth. If the number of bacteria in the oral cavity is high, an unpleasant odor may result [39]. Unfortunately, the tool can only be used to monitor the number of bacteria in the mouth, a proxy for bad breath, but it cannot detect the distinctive odor of the types of gas that makes the mouth smell. This is the background rationale for the making a $\text{Ba}_{0.5}\text{Sr}_{0.5}\text{TiO}_3$ film application which is doped with RuO_2 6% as an Arduino Nano-based odor detection sensor. This tool can monitor bad breath directly by detecting the concentration of sulfurous gases released.

4. Conclusions

The $\text{Ba}_{0.5}\text{Sr}_{0.5}\text{TiO}_3$ film doped with RuO_2 can be used as a bad-breath detecting sensor because it demonstrated a response in the form of voltage changes when exposed to changes in the aroma. The test results demonstrated that $\text{Ba}_{0.5}\text{Sr}_{0.5}\text{TiO}_3$ film doped with RuO_2 with a dope concentration of 6% was the best film of those tested. This film was then applied as the Arduino Nano-based bad-breath detecting sensor. The function of this film is to read bad breath from the types of gas released (sulfur-containing gases produced by naturally occurring bacteria that inhabit the mouth). The use of this tool is very practical, achieved simply by turning on the power on the tool, then blowing over the container shaped like a microphone. The results of bad breath will be displayed on the

16 × 2 LCD. A device housing made of insulating material provides an important safety role for the user.

Author Contributions: Researchers came from the four best universities in Indonesia. In this study, researchers have contributed by following their respective fields. I., B.Y. and F. contributed to the fields of physics and thin film. R.S. contributed in the fields of electronics, hardware and programming. M.Z.F. contributed to the field of chemistry. All authors have read and agreed to the published version of the manuscript.

Funding: This research was funded by USAID through the SHERA program—Centre for Development of Sustainable Regions (CDSR) and Program Penelitian Dasar Unggulan Perguruan Tinggi (PDUPT) DRPM, Republic of Indonesia with grant number 3/E1/KP.PTNBH/2019.

Conflicts of Interest: The authors declare no conflict of interest.

References

- Herawati, D. Mengenali halitosis patologis berdasarkan lokasi asal untuk keberhasilan perawatan Mal-odor Oral. *Majalah Ceramah Ilmiah FKG UGM Yogyakarta* **2003**, *3*, 118–121.
- Djaya, A. *Halitosis: Nafas Tak Sedap*, 1st ed.; Dental Lintas Mediatama: Jakarta, Indonesia, 2000; pp. 2–35.
- McDowell, K.; Denise, K. Halitosis holistik. *Maj. Kedokt. Gigi Dent. Horis.* **2002**, *3*, 30–37.
- Darwis, E.W. Jangan biarkan nafas bau menghambat pergaulan. *J. PDGI* **1997**, *25*, 12–14.
- Preti, G.; Lawley, H.J.; Hormann, C.A.; Cowart, B.J.; Feldman, R.S.; Lowry, L.D.; Young, I.M. Non-Oral and oral aspect of oral malodor. In *Bad Breath Research Perspectives*, 2nd ed.; Rosenberg, M., Ed.; Ramot Publishing-Tel Aviv University: Tel Aviv, Israel, 1997; pp. 149–150.
- Richie, E.; Nani, D.; Pasole, D.; Muhammad, D.; Ade, K.; Johan, I.; Hendradi, H. 'The optical band gap of LiTaO₃ and Nb₂O₅—Doped LiTaO₃ thin films based on Tauc Plot method to be applied on satellite'. *IOP Conf. Ser. Earth Environ. Sci.* **2017**, *54*, 012092–012099.
- Irzaman, Y.; Darvina, A.; Fuad, P.; Arifin, M.; Budiman, M.; Barmawi, M. Physical and pyroelectric properties of tantalum oxide doped lead zirconium titanate [Pb_{0.9950}(Zr_{0.525}Ti_{0.465}Ta_{0.010})O₃] thin films and its application for IR sensor. *Phys. Status Solidi (a) Ger.* **2003**, *199*, 416–424. [[CrossRef](#)]
- Syafutra, H.; Irzaman, H.; Subrata, I.D.M. Integrated visible light sensor based on thin film ferroelectric material BST to microcontroller ATmega8535. *Mater. Sci. Technol.* **2010**, *1*, 291–296.
- Irzaman; Pebriyanto, Y.; Apipah, E.R.; Noor, I.; Alkadri, A. Characterization of Optical and Structural of Lanthanum Doped LiTaO₃ Thin Films. *Integr. Ferroelectr.* **2015**, *167*, 137–145. [[CrossRef](#)]
- Mulyadi, R.; Wahyuni, H. Barium strontium titanate thin film growth with variation of lanthanum dopant compatibility as sensor prototype in the satellite technology. *IOP Conf. Ser. Earth Environ. Sci.* **2018**, *149*, 012069–012076. [[CrossRef](#)]
- Irzaman Syafutra, H.; Rancasa, E.; Nuayi, A.W.; Rahman, T.G.N.; Nuzulia, N.A.; Supu, I.; Sugianto Tumimomor, F.; Surianty Muzikarno, O. The effect of Ba/Sr ratio on electrical and optical properties of Ba_xSr_(1-x)TiO₃ (x = 0.25; 0.35; 0.45; 0.55) thin film semiconductor. *J. Ferroelectr.* **2013**, *445*, 4–17. [[CrossRef](#)]
- Choi, E.S.; Lee, J.C.; Hwang, J.S.; Yoon, S.G. Electrical characteristics of the contour vibration mode piezoelectric transformer with ring/dot electrode area ratio. *J. Appl. Phys.* **1993**, *38*, 5317. [[CrossRef](#)]
- Momose, S.; Nakamura, T.; Tachibana, K. Effects of gas phase thermal decompositions of chemical vapor deposition source molecules on the deposition of BST films. *J. Appl. Phys.* **2000**, *39*, 5384. [[CrossRef](#)]
- Gao, Y.; He, S.; Alluri, P.; Engelhard, M.; Lea, A.; Finder, S.; Melnick, J.; Hance, B. Effect of precursors and substrate materials on microstructure, dielectric properties and step coverage of (Ba, Sr)TiO₃ films grown by metalorganic chemical vapor deposition. *J. Appl. Phys.* **2000**, *87*, 124–132. [[CrossRef](#)]
- Auciello, O.; Scott, J.F.; Ramesh, R. The physics of ferroelectric memories. *Phys. Today* **1998**, *51*, 22–27. [[CrossRef](#)]
- Verma, K.; Sharma, S.; Sharma, D.K.; Kumar, R.; Rai, R. Sol-gel processing and characterization of nanometer-sized (Ba,Sr)TiO₃ ceramics. *Adv. Mater. Lett.* **2012**, *3*, 44–49. [[CrossRef](#)]
- Giridharan, N.V.; Jayavel, R.; Ramasamy, P. Structural, morphological and electrical studies on barium strontium titanate thin films prepared by sol-gel technique. *Crystal Res. Technol.* **2001**, *36*, 65–72. [[CrossRef](#)]
- Chen, X.; Cai, W.; Fu, C.; Chen, H.; Zhang, Q. Synthesis and morphology of Ba(Zr_{0.20}Ti_{0.80})O₃ powder obtained by sol-gel methode. *J. Sol-Gel Sci. Technol.* **2011**, *57*, 149–156. [[CrossRef](#)]

19. Wang, F.; Uusimaki, A.; Leppavuori, S.; Karmanenko, S.F.; Dedyk, A.I.; Sakharov, V.I.; Serenkov, I.T. BST ferroelectric film prepared with sol-gel process and its dielectric performance in planar capacitor structure. *J. Mater.* **1998**, *13*, 1243.
20. Tyunina, M. Dielectric properties of atomic layer deposited thin film barium strontium titanate. *Integr. Ferroelectr.* **2008**, *102*, 29–36. [[CrossRef](#)]
21. Kim, S.; Kang, T.S.; Je, J.H. Structural characterization of laser ablation epitaxial BST thin films on MgO (001) by synchrotron x-ray scattering. *J. Mater.* **1999**, *14*, 2905–2911.
22. Zhu, X.H.; Zheng, D.N.; Peng, J.L.; Chen, Y.F. Enhanced dielectric properties of Mn-doped Ba_{0.6}Sr_{0.4}TiO₃ thin films fabricated by pulsed laser deposition. *Mater. Lett.* **2005**, *60*, 1224–1228. [[CrossRef](#)]
23. Izuha, M.; Ade, K.; Koike, M.; Takeno, S.; Fukushima, N. Electrical properties and microstructure of Pt/BST/SrRuO₃ capacitors. *J. Appl. Phys.* **1997**, *70*, 1405.
24. Lee, J.S.; Park, J.S.; Kim, J.S.; Lee, J.H.; Lee, Y.H.; Hahn, S.R. Preparation of BST thin films with high pyroelectric coefficients in ambient temperatures. *J. Appl. Phys.* **1999**, *38*, L574. [[CrossRef](#)]
25. Irzaman, H.; Darmasetiawan, H.; Hardhienata, H.; Erviansyah, R.; Maddu, A.; Hikam, M.; Arifin, P. Electrical properties of photodiode BST thin film doped with ferrum oxide using chemical deposition solution method. *J. Atom Indones.* **2010**, *6*, 57–62.
26. Irzaman, H.; Syafutra, H.; Darmasetiawan, H.; Hardhienata, H.; Erviansyah, R.; Huriawati, F.; Maddu, A.; Arifin, P. Electrical properties of photodiode Ba_{0.25}Sr_{0.75}TiO₃ (BST) thin film doped with ferric oxide on p-type Si (100) substrate using chemical solution deposition method. *J. Atom Indones.* **2011**, *37*, 133–138. [[CrossRef](#)]
27. Baumert, B.A.; Chang, L.H.; Matsuda, A.T.; Tracy, C.J. A study of BST thin films for use in bypass capacitors. *J. Mater.* **1998**, *13*, 197.
28. Itskovsky, M.A. Kinetics of ferroelectric phase transition: Nonlinear pyroelectric effect and ferroelectric solar cell. *J. Appl. Phys.* **1999**, *38*, 4812. [[CrossRef](#)]
29. Darmasetiawan, H.; Irzaman, H.; Indro, M.N.; Sukaryo, S.G.; Hikam, M.; Bo, N.P. Optical properties of crystalline Ta₂O₅ thin films. *Phys. Status Solidi (a)* **2002**, *193*, 53–60. [[CrossRef](#)]
30. Irzaman, A.; Nuraisah, A.; Aminullah; Hamam, K.A.; Alatas, H. Optical properties and crystal structure of lithium doped Ba_{0.55}Sr_{0.45}TiO₃ (BLST) thin films. *Ferroelectr. Lett. Sect.* **2018**, *45*, 14–21. [[CrossRef](#)]
31. Dahrul, M.; Syafutra, H.; Arif, A.; Irzaman, H.; Indro, M.N.; Siswadi. Synthesis and characterizations photodiode thin film barium strontium titanate (BST) doped niobium and iron as light sensor. In Proceedings of the The 4th Asian Physics Symposium, American Institute of Physics (AIP) Conference, West Java, Indonesia, 12–13 October 2010; Volume 1325, pp. 43–46.
32. Irzaman Dahrul, M.; Yulianto, B.; Hammam, K.A.; Alatas, H. Effects of Li and Cu dopants on the crystal structure of Ba_{0.65}Sr_{0.35}TiO₃ thin films. *Ferroelectr. Lett. Sect.* **2018**, *45*, 49–57. [[CrossRef](#)]
33. Irzaman; Sitompul, H.; Masitoh; Misbakhushudur, M. Optical and structural properties of lanthanum doped lithium niobate thin films. *Ferroelectrics* **2016**, *502*, 9–18. [[CrossRef](#)]
34. Nuayi, A.W.; Alatas, H.; Irzaman, H.; Rahmat, M. Enhancement of Photon Absorption on Ba_xSr_(1-x)TiO₃ Thin-Film Semiconductor Using Photonic Crystal. *Int. J. Opt.* **2014**, *2014*, 534145. [[CrossRef](#)]
35. Hamdani, A.; Komaro, M. A Synthesis of Ba_xSr_(1-x)TiO₃ Film and Characterization Of Ferroelectric Properties and Its Extension as Random Access Memory. *Mater. Phys. Mech.* **2019**, *42*, 131–140.
36. Schwartz, R.W. Chemical solution deposition of perovskite thin film. *J. Chem. Mater.* **1997**, *9*, 2325–2340. [[CrossRef](#)]
37. Endah, K.P.; Rofiqul, U.; Bibin, B.A.; Hidetoshi, S.; Brian, Y.; Husin, A. Micro-Raman analysis of Ba_{0.2}Sr_{0.8}TiO₃ (barium strontium titanate) doped of chlorophyll of cassava leaf. *Ferroelectrics* **2019**, *540*, 227–237.
38. Irzaman; Siskandar, R.; Aminullah; Irmansyah; Alatas, H. Characterization of Ba_{0.55}Sr_{0.45}TiO₃ films as light and temperature sensors and its implementation on automatic drying system model. *J. Integr. Ferroelectr.* **2016**, *168*, 130–150. [[CrossRef](#)]
39. Peverall, R.; Hancock, G. GAD Ritchie. Portable Breath Volatile Organic Compounds Analyser and Corresponding Unit. U.S. Patent 2016/0150995 A1.



Application of Ba_{0.5}Sr_{0.5}TiO₃ (Bst) Film Doped with 0%, 2%, 4% and 6% Concentrations of RuO₂ as an Arduino Nano-Based Bad Breath Sensor

ORIGINALITY REPORT

8%

SIMILARITY INDEX

1%

INTERNET SOURCES

9%

PUBLICATIONS

0%

STUDENT PAPERS

PRIMARY SOURCES

- 1 Irzaman, Ridwan Siskandar, Nida Nabilah, Aminullah, Brian Yulianto, Kholoud Ahmed Hamam, Husin Alatas. " Application of lithium tantalate (LiTaO) films as light sensor to monitor the light status in the Arduino Uno based energy-saving automatic light prototype and passive infrared sensor ", *Ferroelectrics*, 2018

Publication

4%
- 2 Irzaman, Ridwan Siskandar, Aminullah, Irmansyah, Husin Alatas. " Characterization of Ba Sr TiO films as light and temperature sensors and its implementation on automatic drying system model ", *Integrated Ferroelectrics*, 2016

Publication

1%
- 3 Ersin Demir, Hulya Silah. "Development of a New Analytical Method for Determination of Veterinary Drug Oxyclozanide by Electrochemical Sensor and Its Application to

1%

Pharmaceutical Formulation", Chemosensors, 2020

Publication

4

R Estrada, N Djohan, D Pasole, M Dahrul, A Kurniawan, J Iskandar, H Hardhienata, Irzaman. " The optical band gap of LiTaO and Nb O -doped LiTaO thin films based on Tauc Plot method to be applied on satellite ", IOP Conference Series: Earth and Environmental Science, 2017

Publication

1 %

5

Slamet Widodo, M. Miftakhul Amin, Ahyar Supani, Ade Silvia Handayani. "Prototype Design of CO₂, CH₄ and SO₂ Toxic Gas Detectors in the Room Using Microcontroller-Based Fuzzy Logic", Journal of Physics: Conference Series, 2020

Publication

1 %

6

Amalia Sholehah, Diga Fahrezi Faroz, Nurul Huda, Listya Utari, Ni Luh Wulan Septiani, Brian Yulianto. "Synthesis of ZnO Flakes on Flexible Substrate and Its Application on Ethylene Sensing at Room Temperature", Chemosensors, 2019

Publication

1 %

Exclude bibliography On

Application of Ba_{0.5}Sr_{0.5}TiO₃ (Bst) Film Doped with 0%, 2%, 4% and 6% Concentrations of RuO₂ as an Arduino Nano-Based Bad Breath Sensor

GRADEMARK REPORT

FINAL GRADE

/0

GENERAL COMMENTS

Instructor

PAGE 1

PAGE 2

PAGE 3

PAGE 4

PAGE 5

PAGE 6

PAGE 7

PAGE 8

PAGE 9

PAGE 10

PAGE 11
